SMAR 2017 – Fourth Conference on Smart Monitoring,
Assessment and Rehabilitation of Civil Structures

SMAR 2017

Development of anchorage systems for strengthening of steel plates with iron-based shape memory alloy strips

Mohammadreza Izadi[1,2,3], Elyas Ghafoori[1,4], Ardalan Hosseini[1,5], Masoud Motavalli[1,2], Shahrokh Maalek[2]

[1] Empa, Swiss Federal Laboratories for Material Science and Technology, Dübendorf, Switzerland
[2] University of Tehran, Tehran, Iran
[3] ETHZ, Swiss Federal Institute of Technology Zürich, Switzerland
[4] Swinburne University of Technology, Melbourne, Australia
[5] EPFL, Swiss Federal Institute of Technology Lausanne, Switzerland

ABSTRACT: The aim of this study is to propose a series of mechanical anchorage system for strengthening of steel plates with iron-based shape memory (Fe-SMA) strips. Four different friction-based mechanical clamps to anchor the Fe-SMA strips to the steel substrate were designed and tested. A finite element model (FEM) was implemented to perform a stress analysis to optimize the dimensions of each anchorage system. An analytical approach to estimate the load carrying capacity of each clamping system was developed. The results of the analytical and numerical study were then compared with those obtained from experiments. It was found that the performance of the SMA-to-steel joints is mainly dependent on the effective cross-section of the Fe-SMA strip inside the anchorage system as well as the number and the preloading level of the clamp bolts.

1 INTRODUCTION

Iron-based shape memory alloys (Fe-SMAs) are unique materials that have the ability to recover their shape after permanent deformation by heating and subsequent cooling. This interesting behaviour of the material, known as the shape memory effect (SME), enables easy generating of a prestressing in the Fe-SMA material without using the conventional prestressing techniques. If deformed SMA strips are restrained during heating and cooling procedure, a recovery stress is generated inside the material. Recently, a new Fe-SMA, Fe–17Mn–5Si–10Cr–4Ni–1(V,C), in the form of bars and strips has been developed at Empa, Switzerland (Dong et al. 2009). Researchers at Empa have shown that the alloy has a good potential to be used as a prestressing element for civil engineering applications.

Steel structures including buildings, towers, cranes, road and highway bridges are prone to fatigue and corrosion. Advance materials such as carbon fiber-reinforced polymer (CFRP) have been found as a possible method for rehabilitation and strengthening of steel structures. Particularly, prestressing CFRP has been shown to be very effective in enhancement of steel structures capacity (e.g., Ghafoori et al. 2012; Teng et al. 2012; Ghafoori et al. 2015). However, in some cases, prestressing of external CFRP reinforcements is difficult or even impossible (e.g., because of lack of space) as prestressing often requires space and equipment (e.g., hydraulic actuators). Application of Fe-SMAs, however, can provide an easier way of prestressing. As Fe-SMAs will be activated (i.e. prestressed) without any hydraulic actuators and anchor heads, the method will make a prestressing technique easier and therefore more accessible for civil engineering uses. In a new investigation that has been done by Shahverdi et al. (2016) at Empa, this prestressing technique has been conducted successfully on concrete girders.

The first step to utilize the Fe-SMA strips for strengthening of steel plates is to design a suitable retrofit system to anchor the prestressed Fe-SMA strips to the steel plates. Bonded and unbonded solutions already exist to anchor prestressed CFRP strips to the steel substrate, however, adhesively bonding of Fe-SMAs faces some certain problems such as requiring special adhesive for high temperature. On the other hand, unbonded anchorage systems do not have problems related to the long-term behaviour of adhesive when it is subjected to elevated or sub-zero temperatures, humidity and fatigue (Ghafoori et al. 2017).

In the current study, the performance of four different unbonded mechanical anchorage systems for anchoring the Fe-SMA strips to steel plates was evaluated. Numerical simulations were conducted to optimize the geometry of the clamps, while experiments were carried out to determine the total load capacity of each system. The paper is part of the ongoing research on static and fatigue strengthening of steel plate with Fe-SMA strips. In the end, the optimal anchorage system is selected which will be used for static and fatigue strengthening of steel plates.

2 BASIC ENGINEERING DESIGN

The friction coefficient between the Fe-SMA strip and the steel substrate plays the key role in the anchorage system. Thus, the SMA-to-steel friction coefficient was increased by using 3M^{TM} diamond friction shims of grade 10. To calculate the loading capacity, the coefficient of static friction was taken from the product catalogue. Additionally, in the SMA-to-steel joints, thin layers of glass fibre-reinforced polymer (GFRP) laminates were inserted on the top and bottom sides of the Fe-SMA strip to electrically insulate it from the entire assembly. The GFRP laminates were of type high temperature epoxy glass fabric laminate, G-11 type, class H with a thermal class of 180 °C. Moreover, each system consists of a clamp plate that is placed on top of the Fe-SMA strip to distribute the normal pressure generated by the preloaded bolts on the strip. The normal pressure over the Fe-SMA strip is applied based on the maximum admissible preloading force achieved by the ISO metric bolts (with a grade class of 12.9). Figure 1 schematically depicts the application of clamps with their different elements.

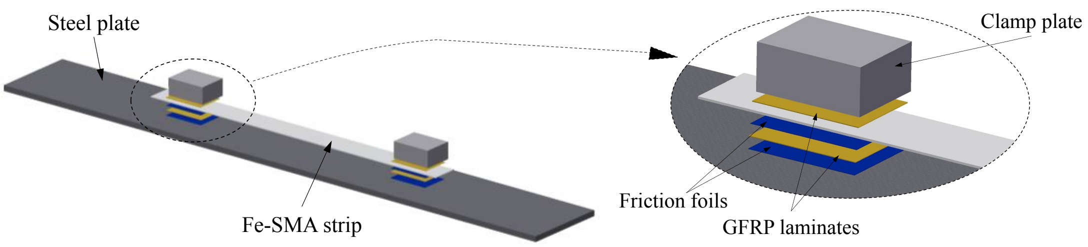

Figure 1. Schematic view of different elements of the SMA-strengthened steel plate.

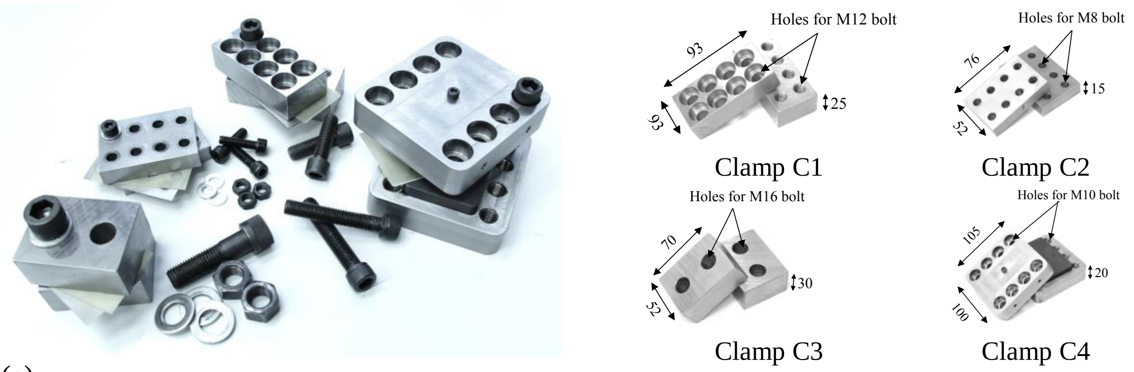

(a) (b)

Figure 2. Four different anchorage systems: (a) different parts of the clamps, (b) dimensions of the clamps (units are in mm).

Four different alternatives are proposed with different geometries and force mechanisms. General information of each clamp is shown in Table 1. In fact, the first three clamps are designed specifically for the SMA-to-steel joints. The last alternative has been developed for the CFRP-to-steel reinforcements by Hosseini et al. (2017). Figure 2 illustrates different parts of the clamps.

Table 1. Four different mechanical anchorage systems.

Clamp Description	Clamp C1	Clamp C2	Clamp C3	Clamp C4
$l \times w \times t$ (mm)	93×43×25	76×52×15	70×52×30	105×100×20
Bolt No. (mm)	M12	M8	M16	M10
Bolt maximum preload (kN)	72	31.1	135.4	49.4
Failure load (kN)	40	50.3	60.6	57

Two different failure modes are likely to limit the static load-carrying capacity of the clamps. The first failure occurs in the first net cross section of the Fe-SMA strip inside the clamp or outside the clamp from gross section (see Figure 3). The second failure mode is attributed to the slippage of the Fe-SMA strip inside the clamping system.

$$F_{failure} = min\{\sigma_{ultimate} \times A_{net} + N \times \mu \times (0.5 \times F_{bolt}),\ F_{ultimate} = A_g \times \sigma_{ultimate}\} \quad (1)$$

where $F_{failure}$ is the total capacity of the SMA-to-steel joint and $\sigma_{ultimate}$ is the ultimate strength of the iron-based SMA strip. Furthermore, A_{net} is the net cross section of strip inside the clamp and N is the number of bolt row. μ is the friction coefficient of the Fe-SMA strip and the steel plate interface, F_{bolt} is the maximum clamping force of one bolt and A_g is the total cross section of the Fe-SMA strip.

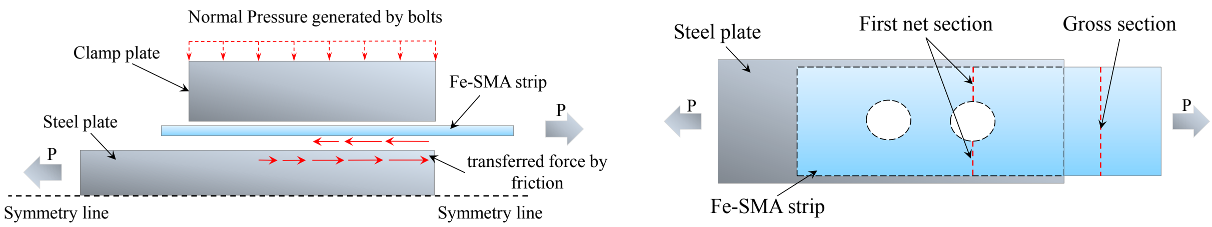

(a) (b)

Figure 3. Mechanism of shear stress transfer between different elements of the clamping system: (a) side view, (b) top view.

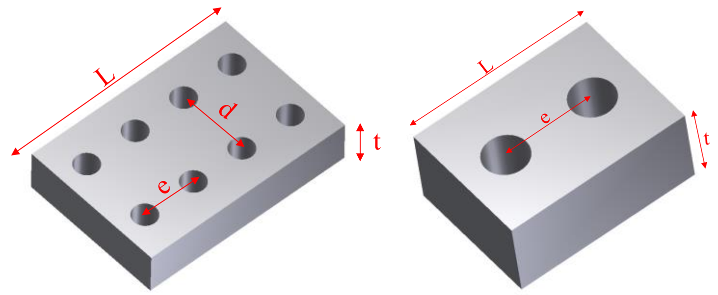

(a) (b)

Figure 4. Geometric variables for parametric study of (a) Clamp C2 and (b) Clamp C3.

3 FINITE ELEMENT SIMULATION

3.1 Finite Element Model description

Finite element (FE) modelling aims to optimize the geometry of the clamps. The FE optimization was performed in a framework of a limited parametric study. The objective of the parametric study was to determine effects of geometric parameters on the distribution of the contact pressure generated by the preloaded bolts over the Fe-SMA strip. Thickness of the clamp plate and the locations of bolts were identified as two important variables (see Figure 4).

Twenty-node quadratic brick elements with reduced integration (C3D20R) were used to mesh the clamp plate, while eight-node linear brick elements with reduced integration (C3D8R) were used for the Fe-SMA strips and the steel plates. A linear material behaviour with a Young's modulus of 200 GPa and a Poisson's ratio of 0.3 was considered for both of the clamp plate and the steel plate. A linear elastic material with a Young's modulus of 170 GPa and Poisson's ratio of 0.3 was assigned for the Fe-SMA strip. A general mesh size of 3.5 mm was used to model the clamp plate, while mesh sizes of 2.5 and 1.5 mm were used for the steel plate and the Fe-SMA strip, respectively. Due to the symmetry of the joint, only a quarter of the whole assembly was modelled. Individual clamp components such as the clamp plate, the Fe-SMA strip and the steel plate were independently modelled and assembled in ABAQUS FE modelling package.

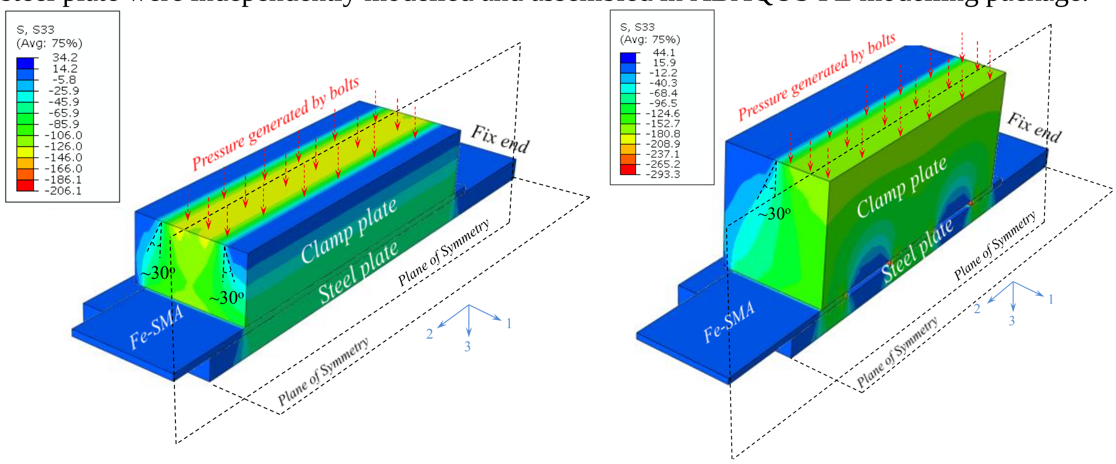

(a) (b)

Figure 5. Results of the FE simulation of Clamps (a) C2 and (b) C3.

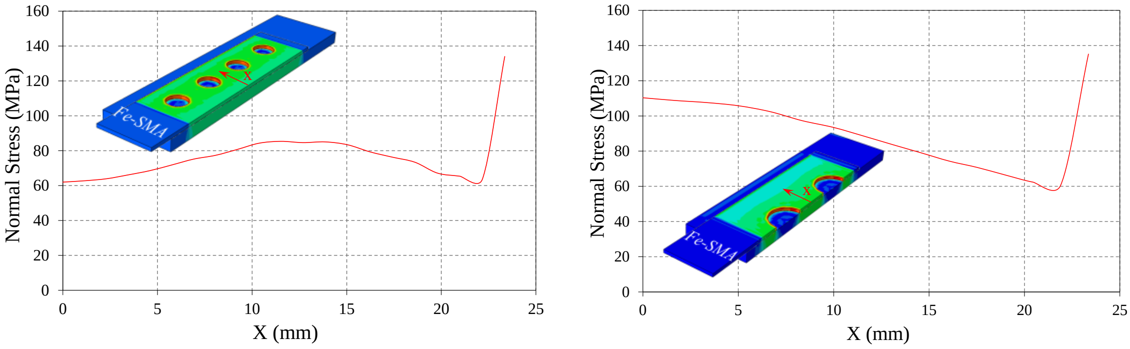

(a) (b)

Figure 6. Normal stress distribution over half width of the Fe-SMA strip for (a) Clamp C2 and (b) Clamp C3.

A "Hard" contact was used for the normal interaction property of different elements, whereas the "penalty" friction technique was incorporated for the tangential contact behaviour. A uniform pressure of 125 and 160 MPa were applied on the clamp plate in Clamps C2 and C3, respectively, to simulate the effect of the bolt preload on the Fe-SMA strip and the steel plate (see Figure 5).

3.2 FE Results

Various FE models for Clamps C2 and C3 with different geometries were created and analysed to find the optimum clamp dimensions. Geometries were optimized based on the homogeneous distribution of the normal stress along the width and the length of the Fe-SMA strip inside the clamp. Furthermore, according to the product catalogue of the friction foils, the contact pressure on the friction foils was recommended to be at least 50 MPa. Figure 6 shows the results of the stress distribution over half width of the Fe-SMA strip for the final configuration of Clamps C2 and C3. Since width of the Fe-SMA strip is smaller than width of the clamp plate, there is a sudden jump in normal stress at edges of the strip.

4 EXPERIMENTS

4.1 Material properties

All the steel components of the clamp including the steel plates and the clamp plates were made of steel grade S355J0 with a nominal yield strength of 355 MPa and a Young's modulus of equal to 200.9 GPa. ISO metric bolts with a grade class of 12.9 have been used to fasten the clamping systems. The friction shims were of type EKagrip®, which were provided by ESK Ceramics GmbH & Co. KG, Germany. Moreover, the GFRP laminates were provided by the Von Roll Deutschland GmbH and the Fe-SMA strips were provided by the re-fer company AG, Switzerland.

4.2 Lap-shear test setup

Clamps C1, C2, and C3 were tested using a horizontal lap shear setup (Figure 7a), however, a vertical test setup was adopted for testing Clamp C4 (Figure 7b). In the horizontal setup, the Fe-

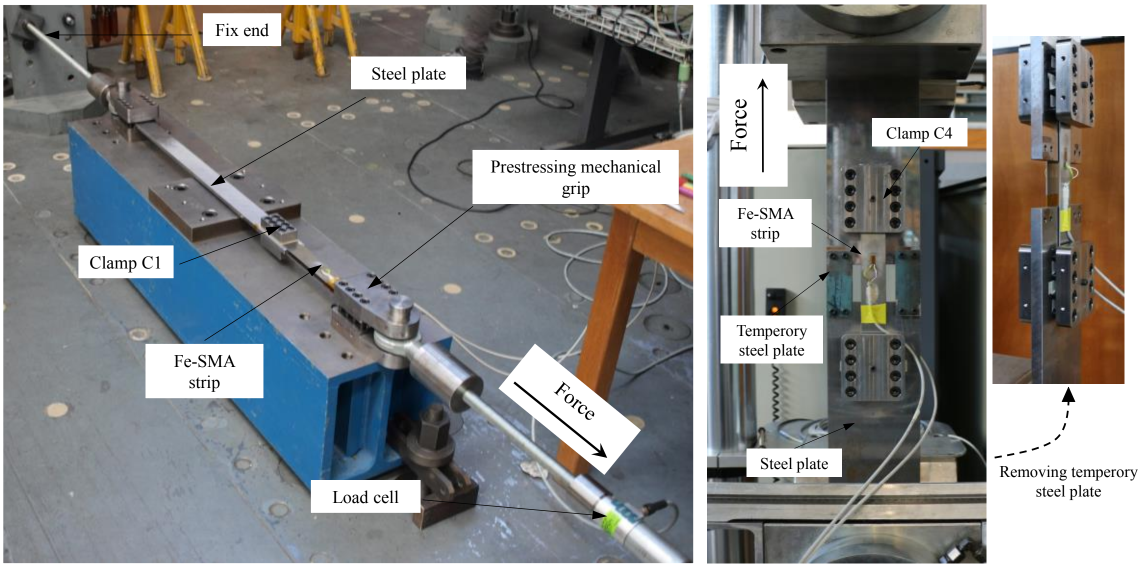

(a) (b)

Figure 7. Lap-shear test setups: (a) horizontal setup using a manual jack, (b) vertical setup using a servo hydraulic cylinder.

SMA strips were fixed inside a mechanical grip, which was connected to a manually operated hydraulic cylinder. A force-controlled loading condition was applied to the whole assembly by increasing the oil pressure. A 300-kN load cell and two strain gauges were used to monitor the load and strain levels in the Fe-SMA strips. In the vertical setup, however, the whole system was placed in a 1000-kN servo-hydraulic testing machine. A quasi-static loading under displacement-controlled condition with a speed of 1 mm/min was applied to Clamp C4.

4.3 Activation test setup

After development and testing of the clamping systems, steel plates were strengthened with the Fe-SMA strips. The Fe-SMA strips were heated with a so-called technique of electrical resistive heating (ERH). An activation test setup, as shown in Figure 8a, was used to thermally activate and therefore prestress the Fe-SMA strips. In order to prevent electricity to flow in the steel plate, the SMA strips were electrically insulated from the steel plate. Therefore, a pair of the GFRP laminates was used on the sides of the Fe-SMA strips, as shown in Figure 1. Several thermocouples were used to monitor the temperature in the Fe-SMA strips and the steel plates.

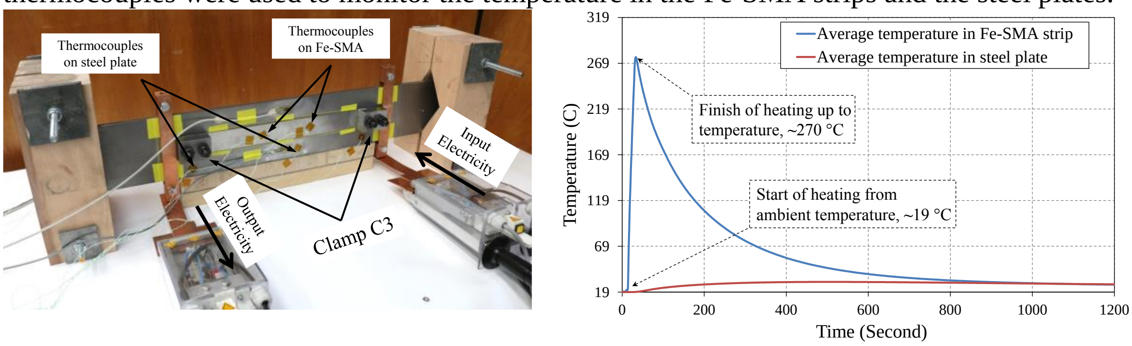

(a) (b)

Figure 8. (a) Insulation test setup, (b) average temperature in the Fe-SMA strip and the steel plate.

5 RESULTS AND DISCUSSIONS

The clamps were loaded in the test setups as explained in section 4.2. Average load vs. strain in the mid-length of the Fe-SMA strip was plotted for all the tested specimens in Figure 9a. The failure mode of the first three clamps was rupture of the Fe-SMA strip from the first row of the holes inside the clamps, as shown in Figure 9b. The rupture occurred due to the stress concentration in the reduced cross section of the Fe-SMA strip inside the anchorage system. The failure mode of the last clamp was rupture of the Fe-SMA outside the clamp in the middle of the SMA strip (see Clamp C4 in Figure 9b). The difference between the results of the failure load capacity of the clamps given in Table 1 with the experimental results might be attributed to the rough estimation of the assumed friction coefficient. It is worth mentioning that $F_{ultimate}$ for Clamp C4 was less than the other clamps since smaller width of the Fe-SMA strip was used for test of Clamp C4. Furthermore, slippage of the clamps was checked visually for all the four anchorage systems and no slippage was observed.

In order to evaluate the insulation of the Fe-SMA strip from surrounding steel components, the Fe-SMA strips were heated up to temperature 270 °C. The temperatures on the Fe-SMA strips and the steel plate were monitored by the thermocouples. As it is illustrated in Figure 8b, the temperature in the steel plate was not increased, indicating that the insulation performed well during heating of the Fe-SMA strips.

6 SUMMARY AND CONCLUSIONS

In the current study, four different friction-based mechanical clamping systems were designed for anchoring the prestressed Fe-SMA strips to the steel substrate. An FE simulation was then utilized to perform a parametric study and optimize the configurations. Furthermore, the load-carrying capacity of the different clamping systems was studied theoretically and experimentally. Experimental results revealed that Clamp C3 is capable of anchoring almost the entire tensile capacity of the Fe-SMA strips to the steel substrate. However, at the same time, it has smaller dimensions compared to Clamp C4. Owing to the high load-carrying capacity and optimized dimensions of Clamp C3, the proposed mechanical clamping system can be considered as a promising technique for static and fatigue strengthening of steel plates using prestressed unbonded Fe-SMA strips. Results of static and fatigue tests on steel plates retrofitted with prestressed Fe-SMA strips will be presented in a future article.

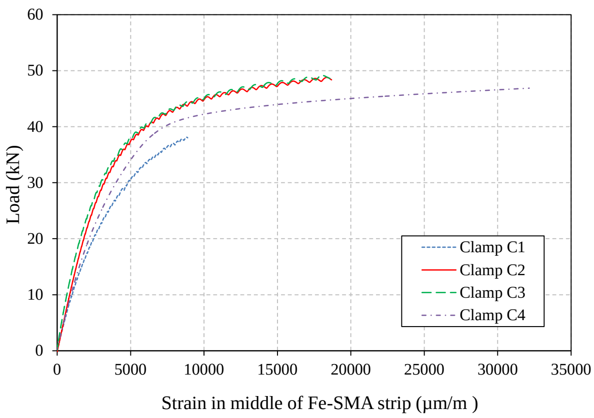

(a)

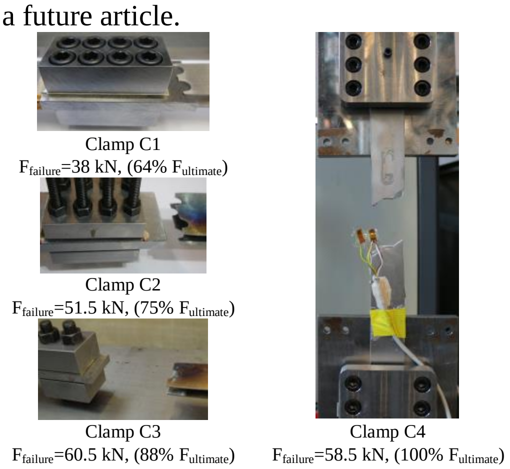

(b)

Figure 9. (a) Load-strain behavior of tested clamps, (b) failure modes.

ACKNOWLEDGMENTS

The first author would like to appreciate the Swiss Federal Commission for Scholarships for Foreign Students (FCS) to provide a Swiss Government Excellence Scholarship to support this project. The support from technicians of the Structural Engineering Research Laboratory at Empa for their exceptional cooperation in performing the experiments is acknowledged. Furthermore, thanks go to the re-fer Company AG, Switzerland and Von Roll Deutschland GmbH to provide Fe-SMA strips and GFRP laminates.

REFERENCES

ABAQUS, S., 2015, Dassault Systémes Simulia Corp., Providence, RI.

Dong, Z., Klotz, UE., Leinenbach, C., Bergamini, A., Czaderski, C., Motavalli, M, 2009, A Novel Fe-Mn-Si Shape Memory Alloy With Improved Shape Recovery Properties by VC Precipitation, *advanced engineering materials*, 11: 40-44.

Ghafoori E., Motavalli M., Botsis J., Herwig A., Galli M, 2012, Fatigue strengthening of damaged metallic beams using prestressed unbonded and bonded CFRP plates, *International Journal of Fatigue*, 44: p. 303-315.

Ghafoori E., Schumacher A., Motavalli M, 2012, Fatigue behavior of notched steel beams reinforced with bonded CFRP plates: Determination of prestressing level for crack arrest, *Engineering Structures*, 45: p. 270-283.

Ghafoori E., Motavalli M, 2015, Innovative CFRP-Prestressing System for Strengthening Metallic Structures, *Journal of Composites for Construction*, 19(6): p. 04015006.

Ghafoori E., Mina D., Hosseini A., Izadi M., Motavalli M, 2017, Recent developments of strengthening techniques for metallic structures, Zurich, Switzerland, *Fourth International Conference on Smart Monitoring, Assessment and Rehabilitation of Civil Structures (SMAR)*, Zurich, Switzerland.

Hosseini, A., Ghafoori, E., Motavalli, M., Nussbaumer, A., Al-Mahaidi, R., Terrasi, G, 2017, A novel mechanical clamp for strengthening of steel members using prestressed CFRP plates, *Fourth Conference on Smart Monitoring, Assessment and Rehabilitation of Civil Structures (SMAR)*, Zurich, Switzerland.

Laminates, VETRONIT G11, Von Roll Deutschland GmbH, D-86199 Augsburg, www.vonroll.com.

Product Information, 3M™ Friction Shims and Coatings, ESK Ceramics GmbH & Co. KG, Germany, info.esk@mmm.com.

Shahverdi M., Christoph C., Philipp A., and Motavalli M, 2016, Strengthening of RC beams by iron-based shape memory alloy bars embedded in a shotcrete layer, *Engineering Structures*, 117: 263–73.

Teng JG., T Yu., and D Fernando, 2012, Strengthening of steel structures with fiber-reinforced polymer composites, *Journal of Constructional Steel Research*, 78: 131-43.